THE CORRECT REPRESENTATION OF OBJECTS MOVING AT RELATIVISTIC SPEEDS

A. SFARTI

387 Soda Hall, UC Berkeley, CA

Received June 10, 2009

In the current paper, we will combine two different disciplines, relativistic physics and 3D graphics in order to derive new results. In a prior paper[14] we have demonstrated the correct representation for object rolling without slipping at relativistic speeds, in the current paper we improve the method and we expand it to the case of translation. To visualize the effects of special relativity, it takes a raytracer. When geometry is moving close to the speed of light with respect to the observer, the geometry appears to be curved: triangles, reflections, shadows and colors change in unexpected ways. Our paper is divided in two main parts, in the first half, we will derive the relativistic equations for arbitrary uniform translation motion and we will make the necessary connections with the physical requirements of a relativistic raytracing algorithm. In the second half, we will demonstrate the effect of the relativistic Doppler shift on the colors wavelengths in the cases of specular and diffuse reflection.

Key words: the appearance of rapidly moving objects, relativistic motion, raytracer program, Hall illumination model, relativistic Doppler effect, specular reflection, diffuse reflection.

PACS: 03.30.+p

1. RAYTRACING FUNDAMENTALS IN COMPUTER GRAPHICS

The process of generating images *via* raytracing involves casting *rays* of light (see Fig. 1) from a *center of projection*, through each *pixel* of a *screen*. Here, the center of projection is equivalent to the focal point of a camera lens, the screen is equivalent to the film used to capture the image and the pixel is the fundamental point element of the film. As seen from Fig.1, not all rays intercept the object.

The condition of ray – object intersection is a necessary (but not sufficient) condition for generating an impression at the pixel location. The sufficient condition is that the *secondary ray* that follows the ideal law of reflection intersects one of the light sources present in the scene. The secondary ray is the ray that makes an angle $\theta_2 = \theta_1$ equal to the angle made by the *primary ray* with the normal **N** to the object (see Fig. 2).

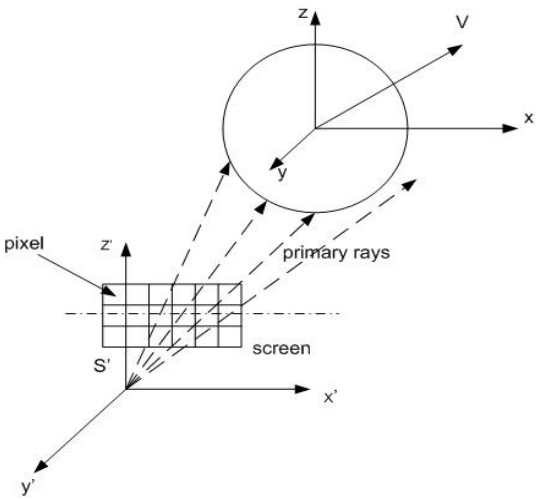

Fig. 1 – Raytracing Fundamentals, Primary Rays.

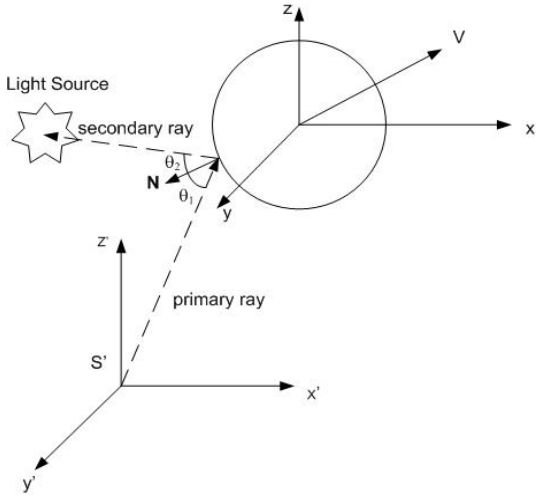

Fig. 2 – Sufficient Condition for Visibility.

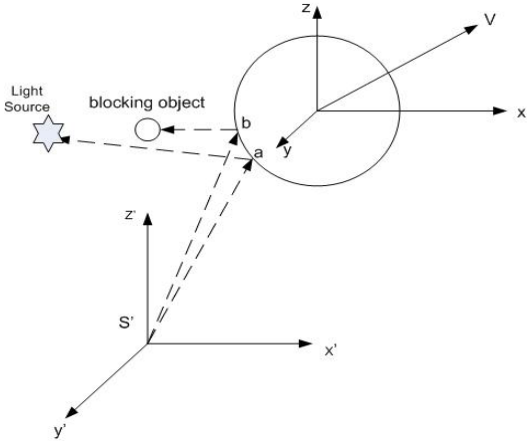

Fig. 3 – Blocked Secondary Rays.

There is the additional condition that the secondary ray is not blocked by any object residing between the point of reflection and the light source (see Fig. 3).

The algorithm, as calculated from the camera frame of reference S', can be summarized as the program:

```
For each pixel (x',y') of the screen
Cast a primary ray
If the primary ray intercepts the object
Cast a secondary ray according to the ideal law of reflection (θ2'=θ1')
If the secondary ray is not blocked and if it intersects a light source
Calculate the illumination for the screen pixel
```

The computation of the illumination for each pixel is done in raytracing *via* the Hall illumination model[8,9]. In this model, the intensity of the reflected light is dependent on the cosine of the angle between the primary ray and the normal **N**. The color of the object is dependent on the spectral distribution of the frequencies.

2. RELATIVISTIC RAYTRACING

We start by deriving the equations for an object that moves along an arbitrary trajectory. In Fig. 1, there are two frames, the co-moving frame S and the *camera* (observer) frame S'. Throughout this paper all the calculations will be reduced to calculations made in S'. We assume that the relative speed between object and camera is **V**.

$$\mathbf{r}' = \mathbf{r} + \mathbf{V}\left(\frac{\gamma - 1}{V^2}\mathbf{r}.\mathbf{V} - \gamma t\right) \tag{2.1}$$

$$t' = \gamma\left(t - \frac{\mathbf{r}.\mathbf{V}}{c^2}\right)$$

$$d\mathbf{r}' = d\mathbf{r} + \mathbf{V}\left(\frac{\gamma - 1}{V^2}d\mathbf{r}.\mathbf{V} - \gamma dt\right) \tag{2.2}$$

We must mark both endpoints of the vector simultaneously in S':

$$dt' = \gamma\left(dt - \frac{d\mathbf{r}.\mathbf{V}}{c^2}\right) = 0 \tag{2.3}$$

The normal **N** to an arbitrary point on the object surface transforms into **N'** according to the rule:

$$\mathbf{N}' = \mathbf{N} + \mathbf{V}\left(\frac{\gamma - 1}{V^2} - \frac{\gamma}{c^2}\right)(\mathbf{N}.\mathbf{V}) = \mathbf{N} + \frac{\mathbf{V}}{V^2}(\gamma^{-1} - 1)(\mathbf{N}.\mathbf{V}) \tag{2.4}$$

N can always be decomposed in a vector parallel with **V** and in one perpendicular on **V**, so that:

$$\mathbf{N'} = \mathbf{N}_{\|} + \mathbf{N}_{\perp} + \frac{\mathbf{V}}{V}(\gamma^{-1} - 1)\mathrm{N}_{\|} = \mathbf{N}_{\perp} + \mathbf{N}_{\|}\gamma^{-1} \tag{2.5}$$

While **N** is a unit vector, **N'** is not, so it needs to be normalized in order to be used in the raytracing computations:

$$\mathbf{N'}.\mathbf{N'} = N^2 - \frac{V^2}{c^2}N_{\|}^{\ 2} = 1 - \frac{V^2}{c^2}N_{\|}^{\ 2} \tag{2.6}$$

In the following calculations we will assume that **N'** has been normalized to unit length. From Fig. 4 we infer immediately that the vector representing the reflected ray **R'** is a function of the normal to the surface **N'** and the vector representing the incident ray **I'**:

$$\mathbf{R'} = \mathbf{N'} + 2\mathbf{I'}\cos\theta = \mathbf{N'} - 2\mathbf{I'}(\mathbf{N'}.\mathbf{I'}) \tag{2.7}$$

It can be easily verified that, if **N'** and **I'** are unit vectors then **R'** is also a unit vector. This is extremely important in the computation of the raytracing illumination model. Furthermore, the point P is considered visible in raytracing if the vector **R'** points towards a light source (see Fig. 2) and is not obstructed by another object (see Fig. 3)

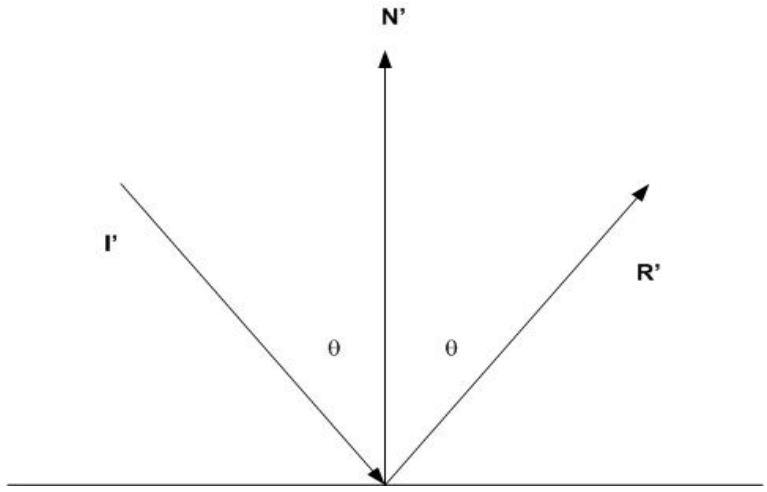

Fig. 4 – Raytracing Vectors.

The process of photographing the moving object from frame S' reduces to taking *snapshots* at regular intervals: $t'_0, t'_0 + \delta, t'_0 + 2\delta, ..., t'_0 + n\delta$. This approach allows us to obtain an animated sequence, *i.e.*, a *motion picture*. Since the object is moving at a very high speed V, we will need to have a very small value for δ in order to avoid the visual effect known as *aliasing*. If we consider all the intersections of the ray

backtracing from the camera all the way to light source as a sequence $\{x_i', y'_i, z_i'\}_{i=1,p}$ where $x_i' = x_i'(t_k')$ and $t'_k = t'_0 + k\delta$ then the final snapshot will be the fused image made of the points that satisfy $|\frac{\sum_{i=1}^{p}\sqrt{\Delta x_i'^2(t_k') + \Delta y_i'^2(t_k') + \Delta z_i'^2(t_k')}}{c} - t_k'| < \varepsilon$ with the ones that satisfy $|\frac{\sum_{i=1}^{p}\sqrt{\Delta x_i'^2(t_{k-1}') + \Delta y_i'^2(t_{k-1}') + \Delta z_i'^2(t_{k-1}')}}{c} - t_k'| < \varepsilon$ where $\Delta x'_i = x_i' - x_{i-1}'$, $i = 1, p$.

3. THE COLOR OF OBJECTS MOVING AT RELATIVISTIC SPEEDS

When objects move at relativistic speeds, we need to re-examine some of the premises in order to take into consideration the relativistic Doppler effect. We will now demonstrate the relationship between the relativistic frequency shift and the perceived color of the moving objects.

The relativistic Doppler effect affects the frequencies as a function of the relative speed between the object and the light source as well as the object and the camera since the object acts a secondary light source by reflecting the incident light. In Fig. 5 f_0 is the frequency emitted by the light source, f_{mirror} is the frequency reflected by the object and $f_{S'}$ is the frequency perceived by the camera. For an object receding from the light source, f_{mirror} is red-shifted from f_0:

$$f_{mirror} = \frac{f_0\sqrt{1-\frac{V^2}{c^2}}}{1+\frac{V}{c}\cos\phi'}, \phi' \in [0, \frac{\pi}{2}] \tag{3.1}$$

On the other hand, because the object is approaching the camera, the frequency $f_{S'}$ is blue-shifted with respect to f_{mirror}:

$$f_{S'} = \frac{f_{mirror}(1+\frac{V}{c}\cos\phi')}{\sqrt{1-\frac{V^2}{c^2}}} \tag{3.2}$$

Combining (3.1) and (3.2) we obtain that there is no frequency shift due to the relative motion between the object and the camera:

$$f_{S'} = f_0 \tag{3.3}$$

Looking at the right-hand side of Fig. 5, for an object receding from the camera and approaching the light source, f_{mirror} is blue-shifted with respect to f_0:

$$f_{mirror} = \frac{f_0\sqrt{1-\frac{V^2}{c^2}}}{1-\frac{V}{c}\cos\phi'}, \phi' \in [\frac{\pi}{2}, \pi] \tag{3.4}$$

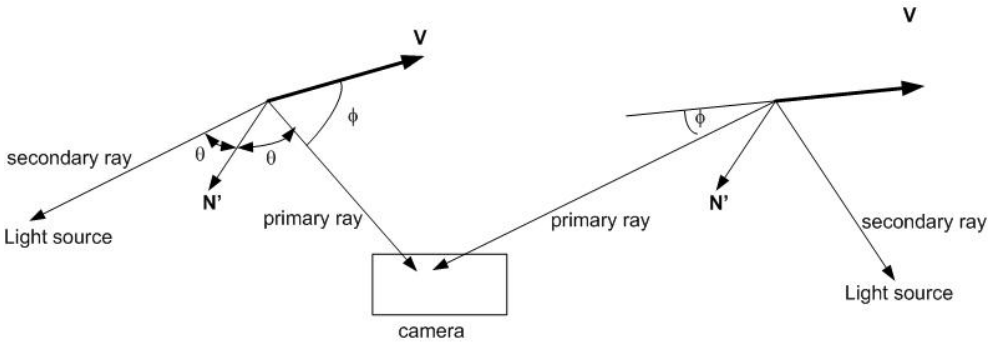

Fig. 5 – Cancellation of the Relativistic Doppler Effect.

On the other hand, because the object is receding from the camera, the frequency $f_{S'}$ is red-shifted with respect to f_{mirror}:

$$f_{S'} = \frac{f_{mirror}(1-\frac{V}{c}\cos\phi')}{\sqrt{1-\frac{V^2}{c^2}}} \tag{3.5}$$

Combining (3.4) and (3.5) we conclude that there is no frequency shift due to the relative motion between the object and the camera for any angle $\phi' \in [0, \pi]$. The above reasoning applies to mirror-like objects that reflect the light coming from the source without changing its frequency. This type of reflection is called *specular* in computer graphics. There is a second type of objects that absorb the incoming spectrum of frequencies and re-emit a selected subset of frequencies. This type of reflection, characteristic to *matte* objects is called *diffuse*. In the case of diffuse reflection, the moving body acts as a secondary light emitter and the perceived frequencies follow the relativistic Doppler effect equations (see Fig. 6). For the object approaching the camera:

$$f_o = \frac{f_{object}(1+\frac{V}{c}\cos\phi')}{\sqrt{1-\frac{V^2}{c^2}}} \tag{3.6}$$

For the object receding from the camera:

$$f_o = \frac{f_{object}(1-\frac{V}{c}\cos\phi')}{\sqrt{1-\frac{V^2}{c^2}}} \tag{3.7}$$

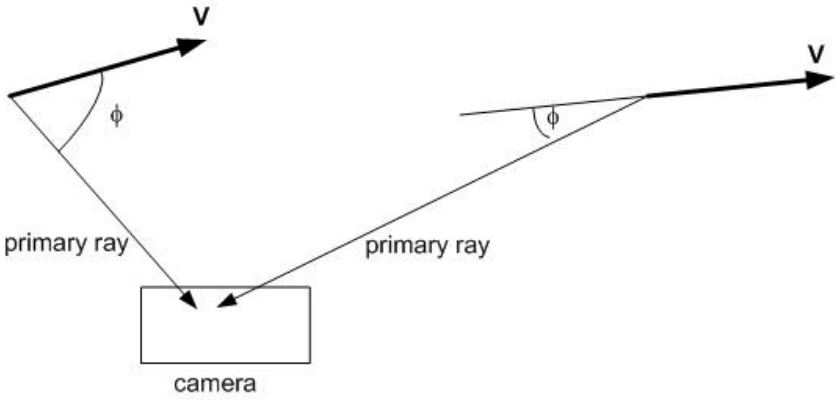

Fig. 6 – Relativistic Doppler Effect for Diffuse Reflection.

When the object is aligned with the camera objective ($\phi' = \pi/2$), we will detect a blue shift consistent with the transverse Doppler effect:

$$f_o = \frac{f_{object}}{\sqrt{1-\frac{V^2}{c^2}}} \tag{3.8}$$

We are taking *snapshots* at regular intervals: $t'_0, t'_1 = t'_0 + \delta, t'_0 + 2\delta, ...$, $t'_k = t'_0 + k\delta$. At each "snapshot" $t'_k = t'_0 + k\delta$ the "shutter" stays open for a time interval $\varepsilon << \delta$. The algorithm can be summarized as:

```
For each pixel (x',y') in the frame "k"
Cast a primary ray
If the primary ray intercepts the object
Cast a secondary ray according to the ideal law of reflection (θ2'=θ1')
If the secondary ray is not blocked and if it intersects a light source
"Fuse" in one image all the pixels that satisfy
```

$$\left|\frac{\sum_{i=1}^{p}\sqrt{\Delta x_i'^2(t_k') + \Delta y_i'^2(t_k') + \Delta z_i'^2(t_k')}}{c} - t_k'\right| < \varepsilon$$

with the ones that satisfy

$$\left|\frac{\sum_{i=1}^{p}\sqrt{\Delta x_i'^2(t_{k-1}') + \Delta y_i'^2(t_{k-1}') + \Delta z_i'^2(t_{k-1}')}}{c} - t_k'\right| < \varepsilon$$

```
Calculate the illumination for the screen pixels that share the same
light path length. Apply the appropriate Doppler effect.
```

If ε is chosen too small, the rendered object will be missing whole parts, if ε is chosen too large then an effect of "motion blur" will result. The latter is much more preferable since motion blur would be expected given the relativistic speeds and since the human brain is much more tolerant to blur than to incomplete renderings. Some experimentation is necessary in terms of determining the optimal value for ε. It is obvious that ε, like δ is a function of the object speed V. Lastly, the computational overhead for calculating the light path length is small, given that the computation is only done for the visible pixels and given that raytracing computations are heavily dominated by ray-object intersections.

4. THE "HEADLIGHT" EFFECT

The "headlight" effect has to do with the increased light intensity **emitted** by object approaching the camera. Exactly as in the case for the blue-shift in the frequency of a diffuse object we derive the energy formula:

$$E_{S'} = \frac{E_{mirror}(1+\frac{V}{c}\cos\phi)}{\sqrt{1-\frac{V^2}{c^2}}} \tag{4.1}$$

where $E_{S'}$ is the light energy as measured in the camera frame S' while E_{mirror} is the energy coming off the approaching object. On the other hand, contrary to what other authors write[13], formula (4.1) is not valid for **specular** surfaces. For the reasons already explained in the previous section, the correct formula for the energy coming off specular objects is simply

$$E_{S'} = E_{mirror} \tag{4.2}$$

5. APPLICATIONS

The most immediate application is in simulating flight at speeds that are a very significant fraction of light speed. As explained earlier[14], at such high speeds motion blur occurs resulting in fusing multiple snapshots in a fashion that makes the objects in the scene impossible to separate. We have countered this naturally occurring effect by scaling down all the speeds by a large factor. In the following images, both the speed of the moving object, V and the speed of light, c have been scaled down by a factor of 1000 in order to limit motion blur without completely

removing it, thus retaining a certain amount of visual realism. Here are a few snapshots taken from our "relativistic speed" flight simulator.

Fig. 7 – Arch Flight-Through.

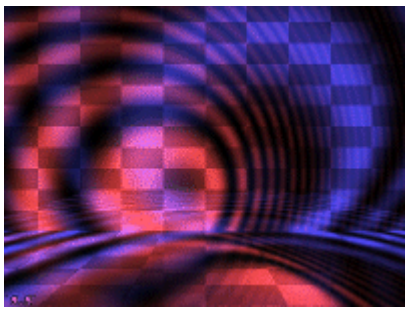

Fig. 8 – Car Headlight Effect.

Figure 7 illustrates the relativistic effects on the geometry of the object while Figure 8 illustrates the effects on color.

6. CONCLUSIONS

We have derived the relativistic equations that describe the *movie* of a rapidly moving object as photographed by a synthetic camera as the ones used in raytracing algorithms for 3D graphics. The relativistic raytracing algorithm has shown the interesting effects of relativistic Doppler effect on the color of the resulting photographs.

REFERENCES

1. J. Terrell, *Invisibility of the Lorentz Contraction*, Phys. Rev. **116,** 1041–1045 (1959).
2. R. Penrose, *The Apparent Shape of a Relativistically Moving Sphere,* Proc. Cambridge Phil. Soc. **55,** 137–139 (1959).
3. M.L. Boas, *Apparent shape of large objects at relativistic speeds*, Am. J. Phys. **29,** 283–286 (1961).
4. E. Sheldon, *The twists and turns of the Terrell Effect*, Am. J. Phys. **56,** 199–200 (1988).
5. J. Terrell, *The Terrell Effect*,Am. J. Phys. **57,** 9–10 (1989).
6. E. Sheldon, *The Terrell Effect: Eppure si contorce*!, Am. J. Phys. **57,** 487 (1989).
7. J.R. Burke, F.J. Strode, *Classroom exercises with the Terrell effect*, Am. J. Phys. **59,** 912–915 (1991).
8. E. Glassner, *An Introduction to Ray Tracing*. Academic Press. (1989).
9. P. Shirley, K. Morley *Realistic Ray Tracing*, 2nd edition. A.K. Peters (2001).
10. M. Pharr, G. Humphreys, *Physically Based Rendering: From Theory to Implementation,* Morgan Kaufmann (2004).
11. V.F. Weisskopf, *The Visual Appearance of Rapidly Moving Objects*, Physics Today **13**(24) (1960).
12. U. Kraus, H. Ruder, D. Weiskopf, C. Zahn, Was Einstein noch nicht sehen konnte – Visualisierung relativistischer Effekte, Physik Journal, **7/8**, (2002).
13. D. Weiskopf, U. Kraus, H. Ruder, *Searchlight and Doppler effects in the visualization of special relativity: A corrected derivation of the transformation of radiance*, ACM Transactions on Graphics **18**(3) (1999).